Thermal Dehydration of Magnesium Hydroxide and Sintering of Nascent Magnesium Oxide

M. Hartman, O. Trnka, and V. Veselý
Inst. of Chemical Process Fundamentals, Academy of Sciences of the Czech Republic,
165 02 Prague 6, Czech Republic

Increasing and constant temperature gravimetric methods were used to measure the thermal decomposition rates of $Mg(OH)_2$ particles. An Arrhenius-type kinetic equation was proposed and tested. Temperature, exposure time on surface area of the calcined particles and other effects of variables were explored. A fractional-order sintering rate expression was developed on the basis of collected experimental data. An integrated model is also presented that considers the surface area generation by calcination and the simultaneous surface reduction caused by sintering of the nascent oxide. Obtained results enable specifying the operating conditions needed for the production of the high surface, reactive magnesium oxide.

Introduction

The kinetics of dehydration and decomposition reactions of various solids such as hydroxides and carbonates are of wide importance due to applications to the preparation of specific materials for catalysts, sorbents and other purposes. Alkaline-earth oxides prepared by the thermal decomposition of alkaline-earth hydroxides under specific conditions can possess some unique properties, including extremely high reactivity and special textural properties. A causal link exists between the low temperature of decomposition of the parent materials and high surface area and high reactivity of their calcines (for example, Hartman and Pata, 1979; Hartman and Svoboda, 1985; Borgwardt, 1989; Mai and Edgar, 1989; Irabien et al., 1990). It is established that the thermal decomposition of $Mg(OH)_2$ particles can produce a high surface MgO product that can react rapidly with SO_2 in waste gas at temperatures of 177–827°C (Kocaefe et al., 1985; 1987). The thermal decomposition of solid substances is accompanied by dramatic changes in important textural properties of the solid such as specific surface area, pore-size distribution and porosity. As a gaseous product evolves in the course of the thermal decomposition, the surface area, as well as the porosity of the solid, are substantially increased.

However, the thermal decomposition is practically always accompanied with the process of sintering of the newly formed solid product. Sintering is usually conceived as a mechanism by which solid grains coalesce at temperatures well below their melting point. In light of the grain theory, micrograins comprise a porous particle produced by thermal decomposition. As micrograin sintering occurs, they grow larger and the surface area is reduced. At high temperature, the sintering process also results in a significant loss of pore volume. These changes degrade the surface area and have an adverse effect on the reactivity of solids with fluids.

Recent studies established that the nature of the parent material, impurities or intentional additions, sintering temperature, sintering time and atmosphere can profoundly influence the rate of the sintering process and, consequently, the properties of the final product (Anderson and Morgan, 1964; Anderson, 1965; Borgwardt and Rochelle, 1990; Milne et al., 1990).

It appears that the sintering takes place at temperatures much lower than suggested by the Tammann temperature, frequently used as an index for the onset of significant lattice mobility. We believe that certain forms of sintering occur even at very moderate conditions such as those for the dehydroxylation of alkaline-earth hydroxides. During the dehydration of hydroxide, two different phenomena can occur simultaneously depending primarily on the humidity and temperature of the gas phase: release of water from the initial reagent due to the reaction and sintering of the decomposed solid (oxide). Research indicates that the produced oxide is the most reactive when a small portion of parent hydroxide remains undecomposed in the reaction product.

Our experience indicates that the problem of sintering cannot be neglected in any gas-solid reaction system. A broad variety of reaction systems range from the processes using presintered

---

Correspondence concerning this article should be addressed to M. Hartman.

particles to situations in which calcination, sintering and other reactions (for example, sulfation) occur on a similar or even on a same time scale.

The decomposition reaction:

$$Mg(OH)_2(s) = MgO(s) + H_2O(g) \tag{1a}$$

is moderately endothermic with $\Delta H^0_{298} = 81{,}060$ J/mol. The temperature dependency of the decomposition heat is approximated by the relationship:

$$\Delta H^0(T) = 78{,}656.0 + 20.146T - 0.04089T^2 \tag{1b}$$

recently proposed by Hartman et al. (1993). The dissociation pressure of magnesium hydroxide at a temperature of interest can be predicted by the simple equation:

$$\ln P^*_{H_2O} = -\frac{9{,}500.0}{T} + 19.6727 \tag{2}$$

also presented in the above work (Hartman et al., 1993). More accurate and more involved expressions for the decomposition heat and the dissociation pressure of magnesium hydroxide and other thermochemical data can be found elsewhere (Hartman and Martinovský, 1992).

Note that thorough crystallographic transformation is involved in the reaction (Eq. 1a). The hexagonal hydroxide lattice is transformed to the face centered cubic lattice of magnesium oxide. Decomposition produces a mass of oxide crystallites that form a porous, spongy relic of the parent hydroxide. Although both parent reactant and product possess only one known crystal structure, the detailed mechanism of the transformation from the standpoint of crystallography is not clear.

The objective of this article is to determine the rate of thermal decomposition of a sample of magnesium hydroxide at moderate temperatures. Some of the important causal relationships involved in the process of evolution and reduction of the specific surface area of nascent magnesium oxide are explored.

Experimental Studies

The experimental work consisted of several parts: sample preparation, careful TGA measurements for the thermal decomposition at increasing temperature, decomposition experiments performed at constant temperature, sintering experiments and measurements of surface area.

Sample preparation

Magnesium hydroxide used in this work was obtained as analyzed reagent grade whose chemical specification is given in Table 1. Sedimentation analysis revealed that the size of the majority of the $Mg(OH)_2$ particles was 4-8 μm. All the particles were in the range of 1 to 50 μm.

A dry sample of magnesium hydroxide in powder form was mixed with some distilled water and the paste was extruded through a coarse sieve. The extrudate formed was dried under vacuum, crushed and sieved. A fraction of the particles selected between the adjacent sieves 0.25 and 0.31 mm was maintained in an airtight container and used in further work. Textural measurements showed that the BET surface area and porosity of these particles of magnesium hydroxide were as large as $S_h = 14$ m^2/g and $e_h = 0.5$, respectively.

Table 1. Chemical Specification of Magnesium Hydroxide

Component	Wt. %
Calcium	0.03
Iron	0.002
Sodium and Potassium	0.004
Sulfate	0.006
Magnesium Hydroxide	97.9
Magnesium Carbonate	2.1
Loss on Ignition at 750°C	31.3

TGA measurements

Decomposition experiments were conducted at a constant rate of temperature increase in the conventional thermogravimetric analysis equipment (Perkin Elmer) at a slow heating rate of 3°C/min. To reduce the possibility of heat-transfer and mass-transfer effects, sample weights were close to 15 mg and nitrogen flow of 70 cm^3/min was maintained through the gas space to ward off the gaseous product of reaction. The size of the sample used was judged to be a reasonable compromise between heat- and mass-transfer intrusions and a relative error in weight measurement. Such conditions ensure that heat- and mass-transfer effects are minimized with intraparticle sample temperature gradients less than 2-4°C.

The decomposition measurements at constant temperature were conducted in a differential reactor. Nitrogen passed through a thin, fixed layer of particles (about 20 mg of hydroxide) at a superficial velocity of 0.3 m/s (Hartman et al., 1987).

Conversions were calculated from the decrease in sample weight, $w_o - w(t)$, at any time and the equation:

$$X = \frac{M_h}{M_w} \cdot \frac{w_o - w(t)}{y\, w_o} \tag{3}$$

where y is the weight fraction of magnesium hydroxide in the original sample, and M_i is the molecular weight of species. Total theoretical conversion ($X = 1, y = 1$) corresponds to $\Delta w / w_o = 0.3089$.

Textural measurements

In large samples, calcined and treated in the differential reactor, physical properties such as BET surface area, pore-size distribution and pore volume were determined. Sintering tests performed with a nitrogen sweep gas followed a similar procedure as for the calcination experiments. The main attention was given to the specific surface area of calcines that was examined with the use of a Micrometrics Digisorb Analyzer.

Kinetics of $Mg(OH)_2$ decomposition

Thermogravimetric analysis provides the data which can serve as a basis for describing the decomposition kinetics under well controlled laboratory conditions. Although extreme care is taken in the experimental work to reduce all presumable side effects, the results obtained are only approximate.

The increasing temperature data are plotted in Figure 1. As

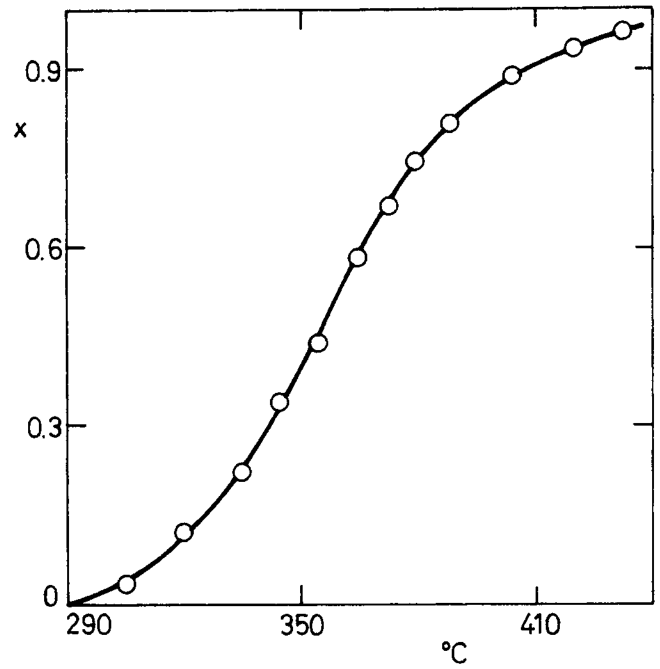

Figure 1. Thermal decomposition of magnesium hydroxide, temperature-increasing method.

Heating rate, 3°C/min; o, experimental data points. Solid line shows the predictions of Eq. 4.

can be seen, the rate of decomposition becomes appreciable at about 290°C. The temperature was increased at a rate 3°C/min to a final temperature of 430°C where decomposition to magnesium oxide was complete.

Experience shows that the thermal decompositions of solids can often be described by the following rate law (Mu and Perlmutter, 1981; Hartman et al., 1987):

$$\frac{dX}{dt} = k_o(1-X)^n \exp(-E/RT) \tag{4}$$

with the initial condition $X(O) = X_i$ and where k_o is the preexponential factor, E is the apparent activation energy, X is the fractional conversion of the decomposing hydroxide to oxide given by Eq. 3 and n is the apparent order of the reaction. Equation 4 is a convenient basis for correlation since it subsumes most of the prior nucleation and diffusion models.

The experimental data accumulated from the temperature increase run were tested empirically by fitting to Eq. 4. Thirty data points at equal temperature intervals were taken to fit this equation. The derivatives dX/dt were approximated as $\Delta X/\Delta t$ and estimated from the conversion measured as a function of time and temperature. The values of the kinetic parameters were computed by the simplex procedure (flexible polyhedron search), using appropriate statistical evaluations for estimating the confidence intervals of the sought parameters. The statistical evaluations are based on the Student "t" distribution. Computational results of the nonlinear regression fitting are given in Table 2.

The computed apparent activation energy is as large as 123.5 kJ/mol. This is between the values of 371.8 and 87.9 kJ/mol reported by Mu and Perlmutter (1981) and Criado and Morales (1976), respectively. The estimated apparent energy of activation is very close to a value of 115.6 kJ/mol, as given by Anderson and Horlock (1962). The calculated apparent order of reaction is $n = 1.73$, which is near the second-order kinetics recommended by Mu and Perlmutter (1981). It differs from the value $n = 1$ employed by Criado and Morales (1976).

Table 2. Kinetic Parameters for Thermal Decomposition of Magnesium Hydroxide (Eq. 4)

Parameter	Value	95% Confidence Interval	Variance
Preexponential Factor, k_o, 1/s	0.1099×10^9	$\pm0.352\times10^3$	0.165×10^{-3}
Order of Reaction, n	0.1728×10	$\pm0.825\times10^{-1}$	0.387×10^{-1}
Activation Energy, E, J/mol	0.1235×10^6	$\pm0.490\times10^3$	0.230×10^3

Equation 4 is highly nonlinear and, therefore, generally sensitive to the variations in values of the kinetic parameters. The conversion computed from this relationship as a function of time at different temperatures is compared to the corresponding measured values in Figure 2. An important point is that the experimental data points shown in this figure were collected from the experiments conducted in the isothermal mode with the use of the differential reactor. As shown in this figure, the predictions and experiment are in reasonable agreement. Note that the different modes of experimental technique are among the important factors affecting this comparison. The decomposition kinetics of magnesium hydroxide can be described by the kinetic expression 4 with the parameters given in Table 2, which were deduced from the increasing-temperature measurements. This corroborates our previous findings with hy-

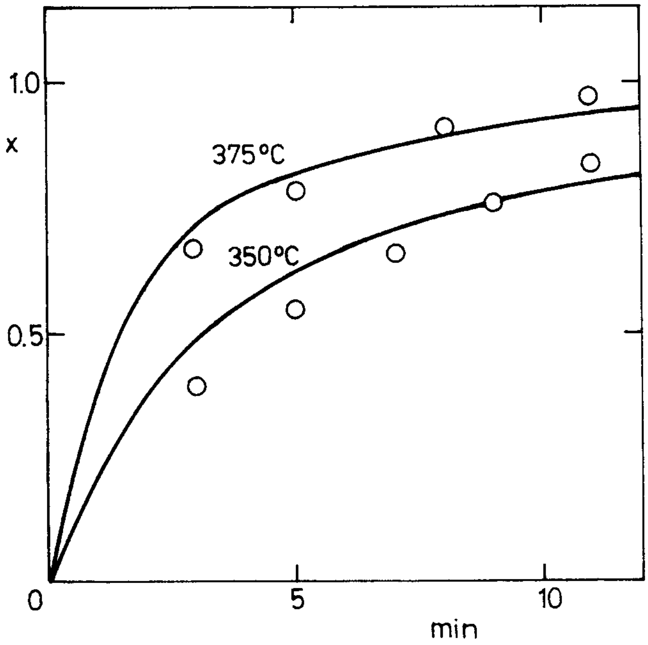

Figure 2. Thermal decomposition of magnesium hydroxide, constant-temperature mode.

o, experimental data points measured at different temperatures. Solid lines show the predictions of Eq. 4 for respective temperatures.

dronium jarosite (Hartman et al., 1987). We believe that Eq. 4 makes it possible to predict in a straightforward manner the rate of dehydroxylation, which would be required to design the performance of a calcination reactor. The empirical correlation developed here has the usual limitations that follow mainly from the experimental conditions from which it was deduced.

Equation 4 is strictly valid for a dry carrier gas. A linear relationship between dehydration rate and partial pressure driving force cannot be generally assumed. However, our common experience shows that the influence of water vapor present in the gas phase on the rate of dehydration can be roughly approximated by introducing a multiplicative factor, z, defined as:

$$z = (P^*_{H_2O} - P_{H_2O})/P^*_{H_2O} \qquad (5)$$

where $P^*_{H_2O}$ is the dissociation pressure of magnesium hydroxide given by Eq. 2 and P_{H_2O} is the partial pressure of water vapor in the gas phase.

Kinetics of sintering

The BET surface area of the particles calcined and sintered in the differential reactor at 350-700°C for 10-180 min are in the range of 75 to 360 m^2/g. The values of surface area are notably higher than those (5-35 m^2/g) measured with the magnesite calcines prepared under similar conditions (Hartman and Svoboda, 1985). Aside from the different parent materials, the presence of impurities (for example, Fe_2O_3, Al_2O_3, TiO_2) in the natural magnesium carbonate has also to be considered in the comparison. The intruded ions cause the lattice defects that facilitate the solid-state diffusion processes. Upon the release of water, the high surface area pseudomorphs, similar to the precursor hydroxide, can exist particularly at a lower temperature. At a high temperature, sintering or recrystallization of magnesium oxide takes place rapidly. The original, hexagonal hydroxide is transformed into the cubic oxide in the course of the thermal decomposition. A variety of the mass-transfer processes which occur during sintering include plastic flow, lattice diffusion, grain boundary diffusion and surface diffusion.

The rate of sintering can also be effected by the gas phase composition (Borgwardt, 1989; Mai and Edgar, 1989). Both carbon dioxide and water vapor tend to accelerate sintering of calcium oxide. This work is concerned primarily with the influence of temperature and time when the effect of carbon dioxide and water vapor is eliminated.

Figure 3 is a plot of the sintering results in a nitrogen flow environment. As can be seen in this figure, the surface area decreases very rapidly with increases in the sintering temperature. Sintering is fast in early stages, but slows down with the time elapsed. At any level of temperature, the surface area remains practically constant for exposure times longer than about two hours. Similar trends were observed in work on sintering of limestone calcines (Hartman and Pata, 1979).

The driving force for sintering is excess surface energy over a certain value which can be attained after very long exposure to a given temperature (Nicholson, 1965). With this assumption, the rate of sintering may be described by:

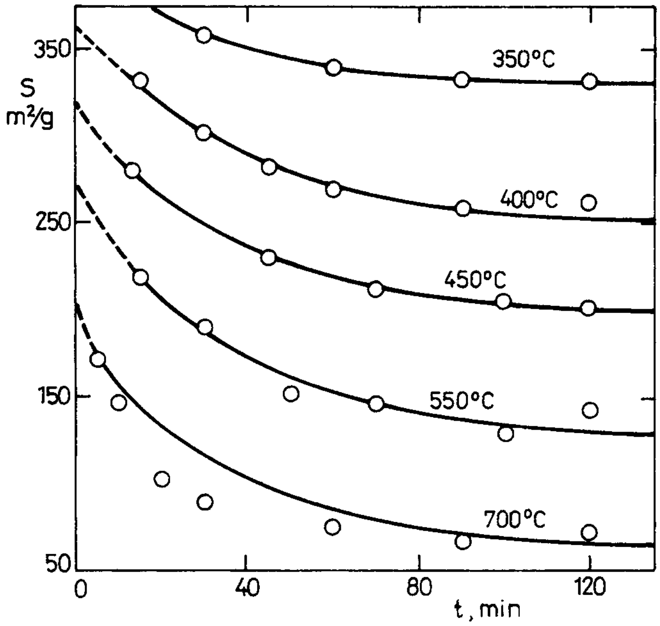

Figure 3. Influence of temperature and exposure time on the surface area of magnesium oxide.

Precursor, magnesium hydroxide; ○, experimental data points measured at different temperatures. Solid lines represent the predictions of Eqs. 6 and 7 for respective temperatures.

$$\frac{dS_c}{d\tau} = -k_s(S_c - S_a)^m \qquad (6)$$

with the initial conditions $S_c(O) = S_i$ and where τ represents the age of elements of magnesium oxide. The sintering rate constant can be expressed as:

$$k_s = A \exp(-E_S/RT) \qquad (7)$$

where A is the preexponential factor, E_S is the apparent activation energy and m is the apparent order of the sintering process. These parameters were established by fitting the experimental data to Eqs. 6 and 7. In this search, the simplex method was employed to minimize the sum of the squares of the differences between experimental and fitted values of surface area. The results of the regression computations yielded the values of A, E_S and m shown in Table 3. Unfortunately, no similar results have been found in the literature for magnesium oxide. Mai and Edgar (1989) described sintering of calcium oxide at temperature about 1,000°C as a second-order

Table 3. Kinetic Parameters for Sintering of Nascent Magnesium Oxide (Eqs. 6 and 7)

Preexponential Factor, A, 1/s	Order of Reaction, m	Activation Energy, E_S, J/mol
0.00810	0.587	5,967.0

Quantity	Min. Value	Max. Value	Variance
$dS_c/d\tau$, $m^2/g \cdot s$	-2.8×10^{-4}	-1.2×10^{-1}	2.3×10^{-3}
$S_c(\tau)$, m^2/g	75.0	363.0	4.9
$S_a(T)$, m^2/g	60.0	260.0	4.9

process with an apparent activation energy as high as 331.6 kJ/mol.

As can be seen in Figure 3, the sintered specific surface area rapidly decreases with increasing temperature from about 360 m^2/g at 350°C to approximately 70 m^2/g at 700°C. An adverse effect of age on the surface area is shown in this figure. The results indicate that the influence of temperature on the surface area is stronger than that of the duration of sintering. An effect of parent material appears to be also significant. The surface area of magnesium oxide prepared from the carbonate precursor (commercial magnesite) at 700°C and sintered for 2 h was 35 m^2/g (Hartman and Svoboda, 1985). This is about half the value shown in Figure 3 for the hydroxide precursor.

The surface area of magnesium oxide can be compared to that of calcium oxide prepared by the thermal decomposition of calcium hydroxide at similar conditions. While the surface areas of calcium oxide formed at 450–700°C and sintered for 30 min amount to 45–20 m^2/g (Irabien et al., 1990), the corresponding values for magnesium oxide are as large as 250–100 m^2/g. Figure 3 also illustrates a good fit between most of the measured values and those predicted by Eqs. 6 and 7. Some differences at 700°C suggest a possible change in the mechanism of sintering at such a high temperature.

In the optimizations performed, the surface area attained after 3 h exposure was taken for the asymptotic surface area at a given temperature. These values are plotted in Figure 4. The reduction of the asymptotic surface area with temperature can be described by the cubic relationship:

$$S_a(T) = 2{,}966.0 - 7.903T + 7.339.10^{-3}T^2 - 2.329.10^{-6}T^3 \quad (\text{for } \tau = 180 \text{ min}) \qquad (8)$$

The initial surface area, S_i, in relation to Eq. 6 is a theoretical concept which can be only imperfectly realized. The values of the initial surface area also shown in Figure 4 are careful extrapolations that may be taken only as approximations. Sensitivity tests have also been performed.

Simultaneous thermal decomposition and sintering

While the surface area is increased by the calcination, it is simultaneously reduced by sintering. The net effect results from the interplay of these opposing phenomena. The rate of the thermal decomposition of magnesium hydroxide has been described by an Arrhenius-type Eq. 4 with an order of reaction of 1.7. The surface area reduction rate of precalcined particles has been correlated by a similar relationship (Eq. 6) in which the difference between the actual and final specific surface area is raised to a power of 0.59. Both Eq. 4 and Eq. 6 are nonlinear ordinary differential equations for X and S_c with time/age as the independent variable and temperature as a parameter. Due to the nonlinearities involved, they have to be integrated numerically.

The two models above are further employed in an effort to describe the process of evolution of the specific surface area of particles during calcination of magnesium hydroxide and subsequent sintering of nascent magnesium oxide.

It is apparent that the total specific area of the solids is a sum of the contributions of both the newly formed magnesium oxide and the remaining, undecomposed magnesium hydroxide:

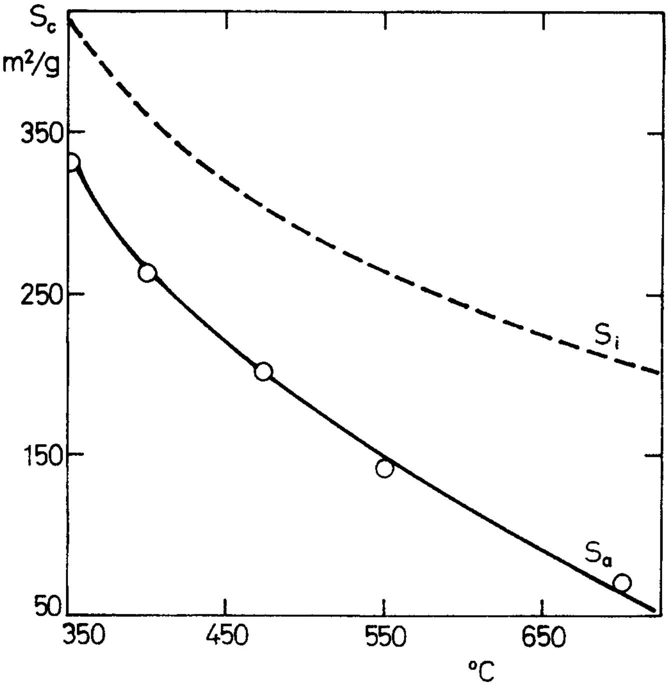

Figure 4. Asymptotic and initial surface area of magnesium oxide as functions of temperature.

Parent material, magnesium hydroxide; o, surface area attained after 180 min of exposure at different temperatures. Dashed line shows extrapolated values.

$$S_t = S(t_c) + (1 + X_c')S_h. \qquad (9)$$

S_h is the specific surface area of magnesium hydroxide and $S(t_c)$ is the total surface of all elements of magnesium oxide with different ages.

At a given moment of time, t_c, a fraction of oxide X is formed. This calcined amount consists of the infinitesimal elements of oxide with different ages that range between zero and t_c. Whereas the age of the single differential element dX is simply introduced as a time elapsed from the moment of its beginning, t with respect to t_c:

$$\tau = t_c - t, \quad t_c \in \langle 0, \infty) \quad t \in \langle 0, t_c \rangle \qquad (10)$$

the spectrum of ages of all the elements depends upon the course of calcination $X = X(t, T)$.

The specific surface area of oxide at the time t_c can be expressed as:

$$S(t_c) = \int_0^{X_c'} S_c(t_c - t) \cdot dX' \qquad (11)$$

or

$$S(t_c) = \int_0^{t_c} \frac{dX'}{dt} \cdot S_c(t_c - t) \cdot dt. \qquad (12)$$

The functions dX/dt and $S_c(t_c - t)$ are given by Eq. 4 and

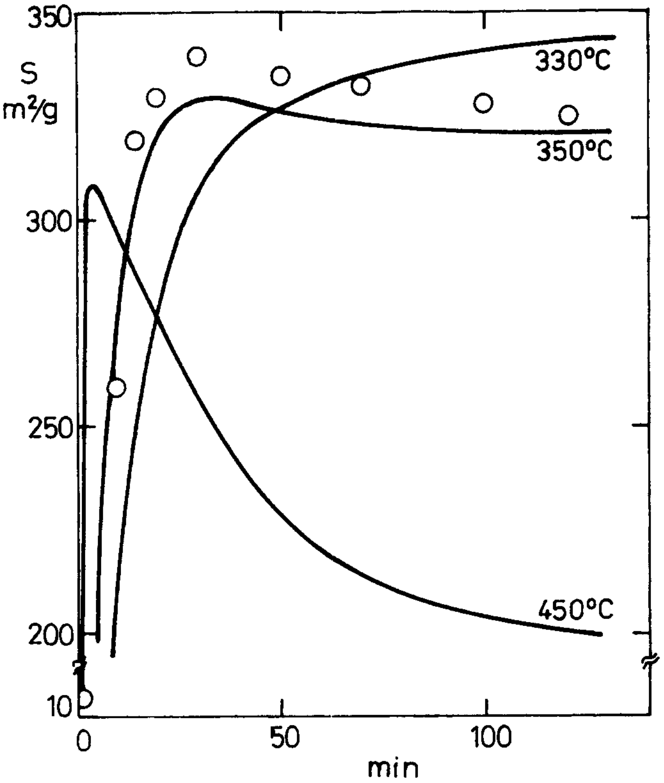

Figure 5. Evolution of the surface area in the course of simultaneous calcination and sintering.

Precursor, magnesium hydroxide; ○, experimental data points measured for 350°C. Solid lines represent the predictions of Eqs. 8 and 11 for respective temperatures.

Eq. 6. The integral on the righthand side of Eq. 12 is evaluated numerically from zero to ever increasing values of t_c.

Note that the conversion X and the specific surface area S are quantities defined on different bases. This inconsistency can be reconciled with the use of the following relationships:

$$X' = \frac{M_c X}{M_c X + M_h(1-X)} \tag{13}$$

$$\frac{dX'}{dt} = \frac{M_c M_h}{[M_c X + M_h(1-X)]^2} \cdot \frac{dX}{dt}. \tag{14}$$

Some predictions of surface area obtained from the calcination/sintering model are presented and compared with the experimental measurements in Figure 5. As can be seen, the model is in reasonable agreement with the experimental results measured at 350°C. As expected, the model predictions and the shapes of the computed curves are particularly sensitive to the operating temperature.

Conclusions

When slowly heated, magnesium hydroxide decomposes in the temperature range of 290 and 410°C. The kinetic expression deduced from the increasing-temperature experiments is in reasonable agreement with the experimental data gathered in the constant-temperature mode.

The surface area of magnesium oxide is affected by the whole temperature history of the calcination/sintering process. It is particularly sensitive to temperature. Even the asymptotic values of the surface area are high, and increase with decreasing temperature from 70 m²/g at 700°C to about 320 m²/g at 350°C.

Experimental results indicate that the sintering, which considerably degrades the surface area, begins at the very moment oxide elements are formed. The proposed model that takes into account simultaneous decomposition of hydroxide and sintering of nascent oxide agrees fairly well with the experimental work.

Acknowledgment

The authors would like to express their appreciation to Mr. A. Martinovský and Mrs. H. Součková for assistance in experimental work. Partial financial support for this study was provided by grant No. 472113 from the Grant Agency of the Czech Academy of Science.

Notation

A = effective frequency factor, fitted parameter, 1/s
E = effective activation energy, fitted parameter, J/mol·K
E_S = effective activation energy of sintering, fitted parameter, J/mol·K
$\Delta H^0(T)$ = standard heat of reaction as a function of temperature, J/mol
k_o = preexponential factor, 1/s
k_s = sintering rate constant, 1/s
m = apparent order of sintering process, fitted parameter
M_c = molecular weight of magnesium oxide = 40.311, g/mol
M_h = molecular weight of magnesium hydroxide = 58.326, g/mol
M_w = molecular weight of water = 18.015, g/mol
n = apparent order of calcination reaction, fitted parameter
P_{H_2O} = partial pressure of water vapor in the gas phase, kPa
$P^*_{H_2O}$ = dissociation pressure of magnesium hydroxide given by Eq. 2, kPa
R = gas-law constant = 8.3144 J/mol·K
S_a = asymptotic specific surface area of magnesium oxide, m²/g
S_c = specific surface area of magnesium oxide, m²/g
S_h = specific surface area of magnesium hydroxide, m²/g
S_i = initial specific surface area of magnesium oxide, m²/g
S_t = total specific surface area of solids, m²/g
t = time, s
t_c = arbitrary moment of time, s
T = temperature, K
X = conversion of magnesium hydroxide to magnesium oxide, mol MgO/[mol MgO + mol Mg(OH)$_2$]
X_c = conversion of magnesium hydroxide to magnesium oxide at $t = t_c$
X' = conversion of magnesium hydroxide to magnesium oxide, g MgO/[g MgO + g Mg(OH)$_2$]
$w(t)$ = mass of Mg(OH)$_2$ − MgO particles at any time, g
w_o = initial mass of dry Mg(OH)$_2$ sample, ($t = 0$), g
y = weight fraction of Mg(OH)$_2$ in initial dry sample, ($t = 0$)
z = correction factor given in Eq. 5
$\tau = t_c - t$ = age of a magnesium oxide element, s
ln = base *e* or natural logarithm

Literature Cited

Anderson, P. J., and R. F. Horlock, "Thermal Decomposition of Magnesium Hydroxide," *Trans. Faraday Soc.*, **58**, 1993 (1962).
Anderson, P. J., and P. L. Morgan, "Effects of Water Vapour on Sintering of MgO," *Trans. Faraday Soc.*, **60**, 930 (1964).

Anderson, P. J., "Some Effects of Water Vapour During the Preparation of Oxide Powders," *Proc. Brit. Ceram. Soc.*, **3**, 33 (1965).

Borgwardt, R. H., "Sintering of Nascent Calcium Oxide," *Chem. Eng. Sci.*, **44**, 53 (1989).

Borgwardt, R. H., and G. T. Rochelle, "Sintering and Sulfation of Calcium Silicate-Calcium Aluminate," *Ind. Eng. Chem. Res.*, **29**, 2118 (1990).

Criado, J. M., and J. Morales, "On the Thermal Decomposition Mechanism for Dehydroxylation of Alkaline-Earth Hydroxides," *J. Therm. Anal.*, **10**, 103 (1976).

Hartman, M., and J. Pata, "Texture of Limestone Calcine and Its Reactivity with Sulfur Dioxide," *Collect. Czech. Chem. Commun.*, **44**, 2465 (1979).

Hartman, M., and K. Svoboda, "Physical Properties of Magnesite Calcines and Their Reactivity with Sulfur Dioxide," *Ind. Eng. Chem. Process Des. Dev.*, **24**, 613 (1985).

Hartman, M., V. Veselý, and K. Jakubec, "Thermal Decomposition and Chemism of Hydronium Jarosite," *Collect. Czech. Chem. Commun.*, **52**, 939 (1987).

Hartman, M., and M. Martinovský, "Thermal Stability of the Magnesian and Calcareous Compounds for Desulfurization Processes," *Chem. Eng. Commun.*, **111**, 144 (1992).

Hartman, M., O. Trnka, and V. Veselý, "Equilibrium Dissociation Pressures and Decomposition Heats of the Magnesian and Calcareous Compounds in Desulfurization Technologies," *Collect. Czech. Chem. Commun.*, **58**, 7885 (1993).

Irabien, A., J. P. Viguri, F. Cortabitarte, and I. Ortiz, "Thermal Dehydration of Calcium Hydroxide," *Ind. Eng. Chem. Res.*, **29**, 1599 (1990).

Kocaefe, D., D. Karman, and F. R. Steward, "Comparison of the Sulfation Rates of Calcium, Magnesium, and Zinc Oxides with SO_2 and SO_3," *Can. J. Chem. Eng.*, **63**, 971 (1985).

Kocaefe, D., D. Karman, and F. R. Steward, "Interpretation of the Sulfation Rate of CaO, MgO, and ZnO with SO_2 and SO_3," *AIChE J.*, **33**, 1835 (1987).

Mai, M. C., and T. F. Edgar, "Surface Area Evolution of Calcium Hydroxide During Calcination and Sintering," *AIChE J.*, **35**, 30 (1989).

Milne, C. R., G. D. Silcox, D. W. Pershing, and D. A. Kirchgessner, "Calcination and Sintering Models for Application to High-Temperature, Short-Time Sulfation of Calcium-Based Sorbents," *Ind. Eng. Chem. Res.*, **29**, 139 (1990).

Mu, J., and D. D. Perlmutter, "Thermal Decomposition of Carbonates, Carboxylates, Oxalates, Acetates, Formates, and Hydroxides," *Thermochim. Acta*, **49**, 207 (1981a).

Mu, J., and D. D. Perlmutter, "Thermal Decomposition of Inorganic Sulfates and Their Hydrates," *Ind. Eng. Chem. Process Des. Dev.*, **20**, 640 (1981b).

Nicholson, D., "Variation of Surface Area During the Thermal Decomposition of Solids," *Trans. Faraday Soc.*, **61**, 990 (1965).

Manuscript received Mar. 29, 1993, and revision received July 1, 1993.